Flash Drought Dynamics in China's Major Agricultural Plains: Spatiotemporal Patterns and Crop Photosynthetic Recovery Across Cropping Systems

Shuo Mao †, Mengzhen Han †, Hao Chen †, Shaowei Ning *, Zhenyu Zhang *, Le Chen, Yuliang Zhou, Weimin Ju

Posted Date: 19 May 2026

doi: 10.20944/preprints202605.1263.v1

Keywords: flash drought; solar-induced chlorophyll fluorescence; gross primary productivity; cropping systems; spatiotemporal evolution; photosynthetic recovery

 doi:10.20944/preprints202605.1263.v1

Article

Flash Drought Dynamics in China's Major Agricultural Plains: Spatiotemporal Patterns and Crop Photosynthetic Recovery Across Cropping Systems

Shuo Mao [1,†], Mengzhen Han [1,†], Hao Chen [1,†], Shaowei Ning [2,*], Zhenyu Zhang [1,*], Le Chen [2], Yuliang Zhou [1] and Weimin Ju [3]

[1] School of Resource and Environmental Engineering, Hefei University of Technology, Hefei 230009, China
[2] College of Civil Engineering, Hefei University of Technology, Hefei 230009, China
[3] International Institute of Earth System Science, Nanjing University, Nanjing 210023, China
* Correspondence: ning@hfut.edu.cn (S.N.); 2024800044@hfut.edu.cn (Z.Z.)
[†] These authors contributed equally to this work.

Highlights

What are the main findings?

- The southern Middle-Lower Yangtze Plain exhibited a "high-frequency–low-intensity" flash drought pattern, while the central North China Plain showed a "low-frequency–high-intensity–long-duration" pattern, with rice systems facing high-frequency shock risks and rainfed/rotation systems bearing intensity-cumulative risks across China's major agricultural plains during 2001–2024.
- SIF responded to flash droughts 6–9 days earlier than GPP across all cropping systems, revealing a consistent "rapid physiological response–lagged carbon assimilation recovery" pattern, with the month of occurrence, drought duration, and decline rate identified by Random Forest–SHAP analysis as the dominant drivers of photosynthetic recovery.

What are the implications of the main findings?

- The systematic 6–9 day lead time of SIF over GPP, confirmed across diverse cropping systems, establishes SIF as a reliable remote sensing-based early warning indicator that can support proactive agricultural drought response well before conventional vegetation productivity declines become detectable.
- The crop-specific risk differentiation and the dominant role of phenological timing over drought intensity provide a scientific basis for designing targeted, system-specific mitigation strategies, optimizing rotation scheduling (e.g., shortening fallow intervals in WW-SSR systems), and enhancing regional food security management under intensifying climate extremes.

Abstract

Flash drought, as a rapidly developing form of drought, has become an increasing threat to agricultural production, ecosystem stability, and regional carbon cycling, particularly in croplands within monsoon regions. Existing studies have mainly focused on point-scale identification or conventional vegetation indices, while a systematic understanding of the regional spatiotemporal evolution of flash droughts and crop-specific differences in photosynthetic recovery remains limited. Using multi-source remote sensing data from the North China Plain and the Middle-Lower Yangtze Plain during 2001–2024, this study integrated triple collocation error assessment, root-zone soil moisture percentile-based identification, connected component tracking, and Random Forest–SHAP analysis to characterize flash drought trajectories and their impacts on vegetation. The results showed that the southern Middle-Lower Yangtze Plain exhibited a high-frequency but low-intensity pattern, whereas the central North China Plain was characterized by relatively low frequency but higher

 doi:10.20944/preprints202605.1263.v1

intensity and longer duration. Rice-based systems were more vulnerable to frequent flash drought shocks, while rainfed and rotation systems faced stronger cumulative risks. Solar-induced chlorophyll fluorescence (SIF) responded to flash droughts 6–9 days earlier than gross primary productivity (GPP), and all cropping systems exhibited a "rapid physiological response–lagged carbon assimilation recovery" pattern. The month of occurrence, drought duration, and decline rate were identified as the dominant factors controlling photosynthetic recovery. These findings extend the flash drought monitoring framework from the perspectives of regional connectivity and crop recovery mechanisms, and provide a remote sensing-based scientific basis for agricultural early warning, drought mitigation, and food security management.

Keywords: flash drought; solar-induced chlorophyll fluorescence; gross primary productivity; cropping systems; spatiotemporal evolution; photosynthetic recovery

1. Introduction

As one of the most pervasive meteorological disasters, drought has long posed a persistent threat to agricultural production, ecosystem stability, and regional carbon budget balance. Conventional droughts typically develop at a gradual pace, often requiring several months or even years to progress from onset to peak intensity [1]. In recent years, with the rising evaporative demand and intensifying atmospheric desiccation [2], both the frequency and the rate of drought progression have continued to increase, and a novel drought paradigm—flash drought—has emerged as an increasingly important subject in drought research [3]. Compared to conventional droughts, flash droughts can induce rapid soil moisture depletion, evapotranspiration imbalance, and a concurrent surge in vapor pressure deficit (VPD) within a few weeks, thereby imposing more severe impacts on agricultural production and ecosystem functioning [4,5]. During the summer of 2013, flash droughts occurred successively in 13 provinces of southern China within less than a month, leading to damage to over 2 million hectares of crops [6]. The North China Plain, as one of the nation's principal grain-producing regions, is frequently subjected to severe agricultural droughts during both the spring and autumn seasons, with spring drought intensity generally exceeding that of autumn. Therefore, the accurate identification of flash drought events and the elucidation of their spatiotemporal evolution patterns are of considerable theoretical and practical significance for regional drought risk assessment and food security safeguards.

At present, a universally accepted definition of flash drought has yet to be established in the scientific community, and a diverse suite of indices has been developed for flash drought identification, primarily including the Evaporative Stress Index (ESI) [7], Evaporative Demand Drought Index (EDDI)[8], the combination of Standardized Evaporative Stress Ratio (SESR) [9] and Rapid Change Index (RCI) [10], as well as soil moisture (SM) [11]. Previous studies have demonstrated that soil moisture anomalies serve as reliable indicators during the initial phase of drought, and are particularly suitable for flash drought monitoring [2,12]. The rapid decline in soil moisture can function as a critical precursory signal for flash drought occurrence. Osman et al. compared the performance of key variables including precipitation (P), root-zone soil moisture (RZSM), temperature (T), and actual versus potential evapotranspiration in flash drought identification, and found that RZSM exhibited the most distinct response signal to flash droughts. However, existing soil moisture-based drought monitoring studies have predominantly focused on the onset and termination of drought at the point scale, emphasizing the temporal persistence characteristics of drought, with the run theory being the most commonly employed approach [13,14]. Such studies generally overlook the spatial connectivity and regional synchronicity of drought, which may substantially underestimate the actual extent and severity of regional drought, consequently leading to inadequacies in drought response and risk management. To address this limitation, a series of innovative methods, such as hydrological models [15], machine learning [4] , and complex networks [16] have been progressively applied to research on drought propagation and evolution.

 doi:10.20944/preprints202605.1263.v1

Among these, three-dimensional spatial connectivity analysis can precisely characterize the spatiotemporal dynamics of short-duration, regional flash drought events by identifying spatially contiguous drought clusters [17,18].

During flash drought episodes, high temperatures and scarce precipitation induce a rapid rise in VPD, forcing stomatal closure in vegetation, suppressing CO_2 uptake and photosynthetic carbon fixation, and consequently leading to a significant decline in terrestrial ecosystem productivity [19,20]. Compared to deep-rooted vegetation, shallow-rooted vegetation (particularly crops) is more sensitive to flash droughts, and existing studies have predominantly employed conventional remote sensing vegetation indices, including the Normalized Difference Vegetation Index (NDVI) and Leaf Area Index (LAI), to assess vegetation response patterns to drought [21]. Nevertheless, these vegetation indices exhibit a notable lag in their response to flash droughts, making it difficult to promptly and timely capture the impacts of flash droughts on vegetation physiological processes [23,24]. To overcome this limitation, recent research has increasingly shifted toward the direct observation of vegetation functional indicators [24,25]. Among these, Gross Primary Productivity (GPP) is a key indicator for characterizing ecosystem carbon sequestration capacity and carbon cycling processes, and is sensitive to drought stress [26]. With advances in remote sensing technology, Solar-Induced chlorophyll Fluorescence (SIF), as a direct proxy for the light reaction phase of photosynthesis, has also been widely utilized for monitoring vegetation physiological status and rapid drought response. Compared to conventional vegetation indices, SIF can reflect the physiological signals of photosynthetic system suppression at an earlier stage under conditions of stomatal closure and rapidly rising VPD, typically preceding the decline in GPP by several weeks, and is thus considered an important early indicator of drought, particularly flash drought [27]. Previous studies have shown that SIF and GPP exhibit high consistency at interannual and seasonal scales across multiple ecosystems; however, under drought stress, significant differences exist between the two in terms of response magnitude, temporal characteristics, and sensitivity [28,29] . However, current research on SIF and GPP has largely been concentrated on natural ecosystems or vegetation at the aggregate scale [30,31] , with relatively insufficient attention to cropland ecosystems, and most studies have focused on yield impacts [32] while lacking fine-scale comparative analyses based on different crop types. Meanwhile, the vegetation response to drought is modulated by intrinsic drought characteristics such as intensity, frequency, and duration [33–35]. Yet most of the relevant findings have been derived from studies of conventional droughts, and how multi-factor interactions affect vegetation photosynthetic processes under the rapid, intense stress scenarios characteristic of flash droughts remains unclear.

Therefore, building upon existing research, this study employs multi-source remote sensing data (Solar-Induced chlorophyll Fluorescence SIF, soil moisture data, and GPP data), integrated with the root-zone soil moisture percentile method and connected component analysis, to systematically investigate the spatiotemporal distribution of flash drought events and their impacts on vegetation recovery across different cropping systems in the North China Plain and the Middle-Lower Yangtze Plain. Concurrently, a Random Forest model combined with SHAP (Shapley Additive Explanations) values is utilized to quantitatively evaluate the driving factors of photosynthetic recovery rate, with the aim of bridging the existing gaps in research on regional flash drought emergency response mechanisms and crop recovery capacity assessment. This study is expected to contribute to the theoretical understanding of drought response mechanisms while also offering practical implications for regional agricultural disaster prevention and mitigation, and to provide novel scientific evidence for future drought prediction, food security management, and ecosystem stability assessment.

2. Materials and Methods

2.1. Study Area

Under the context of global warming, the increasing frequency of extreme high-temperature events and intensified land-atmosphere interactions have led to a significant upward trend in flash

 doi:10.20944/preprints202605.1263.v1

drought occurrences across East Asia [36]. Within the East Asian monsoon region of China, the North China Plain and the Middle-Lower Yangtze Plain represent the nation's typical rainfed agricultural zone and major rice-producing area, respectively, serving as core regions for national food security that are highly sensitive and vulnerable to climate change. Accordingly, this study selected the North China Plain (34°–40°N, 110°–120°E) and the Middle-Lower Yangtze Plain (28°–33°N, 110°–122°E) as representative study areas (Figure 1(a)), to elucidate the spatiotemporal characteristics and driving mechanisms of flash droughts under the East Asian monsoon climate.

The two plains are geographically extensive, span a wide latitudinal range, and feature diverse cropping structures. Following the classification by Yang (2025) et al., the land use categorization of the study area is illustrated in Figure 1(c). Specifically, SSR denotes single-season rice, DSR denotes double-season rice, WW denotes winter wheat, WW-SSR denotes winter wheat–single-season rice rotation, M denotes maize, and WW-M denotes winter wheat–maize rotation.

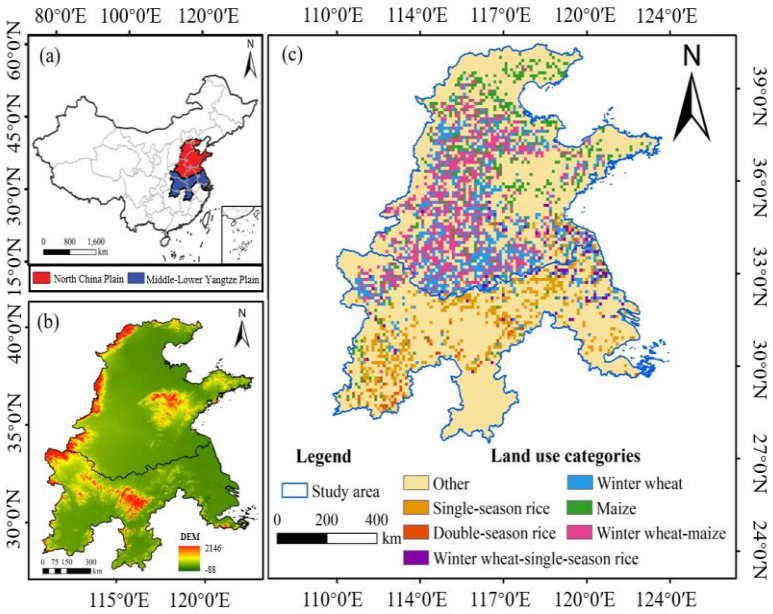

Figure 1. Geographical location of the study area (a), digital elevation model (b) and spatial distribution of land use types (c).

2.2. Data Sources

The datasets employed in this study are summarized in Table 1, and detailed descriptions and preprocessing procedures are provided in the Supplementary Materials S1. All the aforementioned datasets were uniformly resampled to a spatial resolution of 0.1°.

Table 1. Detailed Information of the Employed Data.

Poducts	Spatial coverage	Temporal coverage	Resolution	Data source
ERA5-Land	Global	1950-present	1d/0.1°	https://cds.climate.copernicus.eu/cdsapp#!/dataset/reanalysis-era5-land?tab=overview
GLEAM v4.2	Global	1980-2024	1d/0.1°	https://www.gleam.eu/
SMCI1.0	China	2000-2022	1d/0.09°	https://poles.tpdc.ac.cn/
GOSIF	Global	2000-2024	8d/0.05°	https://globalecology.unh.edu/data/GOSIF.html
GOSIF GPP	Global	2000-2024	8d/0.05°	https://globalecology.unh.edu/data/GOSIF-GPP.html

 doi:10.20944/preprints202605.1263.v1

CCD	China	2001-2024	1year/30 m	https://www.scidb.cn/en/detail?dataSetId=9df1ab40944b4ce58eec7265462b4247&version=V1&code=o00119

2.3. Methods

2.3.1. Multi-Source Soil Moisture Error Assessment (Triple Collocation)

Considering that the regional performance of different soil moisture products may be affected by vegetation, soil type, and underlying surface conditions, the Triple Collocation (TC) method [37] was adopted in this study to objectively assess data quality by constructing a triplet from ERA5, GLEAM, and SMCI1.0 datasets, thereby quantitatively estimating the random error, signal-to-noise ratio, and bias characteristics of each dataset independent of observational ground truth (Figure 2). The TC method has been widely employed for accuracy evaluation and intercomparison of multi-source soil moisture data at both global and regional scales, and can effectively identify datasets with high accuracy and low uncertainty [38,39] . Detailed computational procedures and formulas can be found in the work of McColl et al. [40]. Table S1 in the Supplementary Materials presents the correlation coefficients and standard noise errors computed via the TC method for each dataset; all three datasets exhibited relatively low noise errors, with the ERA5 dataset achieving the highest correlation coefficient and the best overall performance, and therefore ERA5-Land was selected as the data source for subsequent flash drought identification in this study.

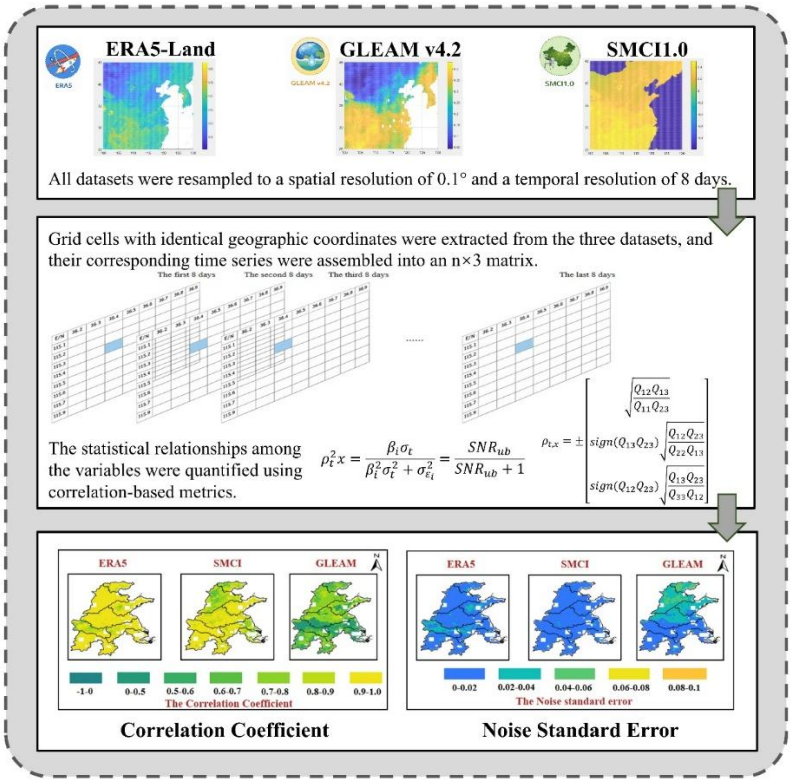

Figure 2. Workflow for multi-dataset integration and uncertainty assessment based on triple collocation analysis.

2.3.2. Flash Drought Identification

This study adopted the internationally recognized flash drought identification framework proposed by Yuan et al. [41,42], with flash drought events extracted based on RZSM percentiles. To eliminate the climatological and seasonal discrepancies in soil moisture across different regions, the

 doi:10.20944/preprints202605.1263.v1

Empirical Distribution Function (EDF) was employed to calculate RZSM percentiles [41,43,44]. For each grid cell, a multi-year RZSM time series was constructed using a 17-day window centered on the target date p (from p−8 to p+8), followed by EDF fitting to map RZSM values onto a 0–100 percentile scale.

The specific criteria for flash drought identification are as follows:

a) A flash drought commences when the RZSM percentile declines from ≥40% to ≤20%.

b) A flash drought terminates when the RZSM percentile recovers to >20%.

c) The mean decline rate over an 8-day interval is ≥8%.

d) The drought duration is ≥24 days (i.e., ≥3 octad periods).

2.3.3. Spatiotemporal Trajectories of Flash Droughts

The analytical workflow for spatiotemporal trajectory analysis of flash droughts is illustrated in Figure 3: RZSM percentiles were first computed from ERA5 reanalysis data to identify flash drought events at the grid scale; spatially contiguous drought patches were then extracted through connected component analysis; a temporal matching algorithm was applied to link discrete patches into continuous spatiotemporal drought events, thereby constructing a flash drought trajectory database; on this basis, the centroid migration paths and three-dimensional propagation characteristics of flash droughts were analyzed [45]. A composite flash drought intensity index was constructed by integrating flash drought frequency, duration, and intensity. This study selected the two largest-scale typical flash drought events based on the composite intensity index across two years, analyzed their spatial displacement distances and propagation characteristics, and ultimately derived the spatial pattern of drought propagation timing.

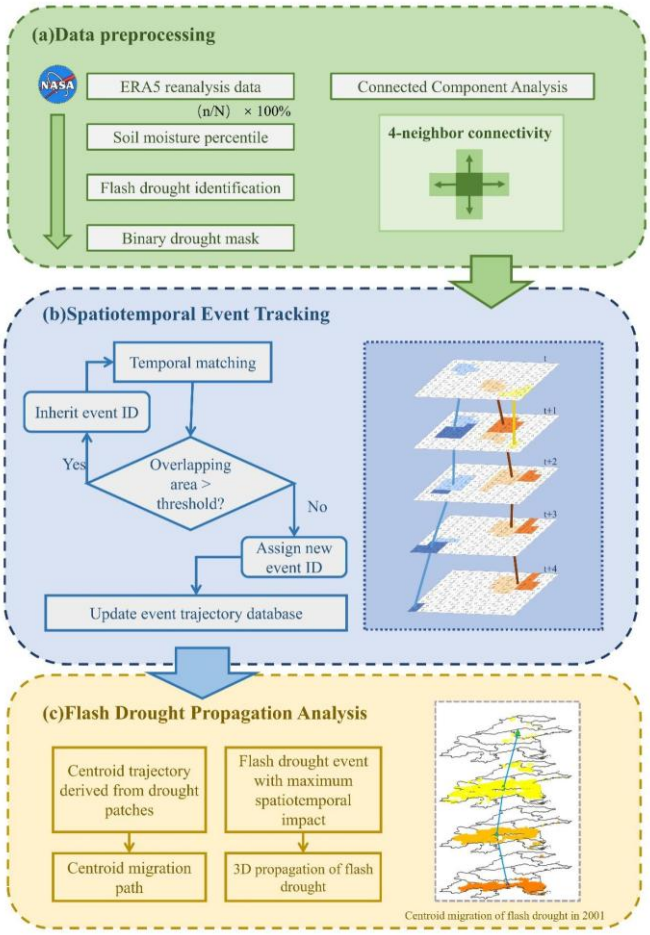

Figure 3. Workflow for identifying and tracking flash drought events based on soil moisture percentiles and spatiotemporal connectivity.

 doi:10.20944/preprints202605.1263.v1

2.3.4. Analysis of Vegetation Photosynthetic Response and Recovery

This study employed two remote sensing-based vegetation productivity indicators (VP), namely GPP and SIF, to characterize the dynamic response of ecosystems to flash droughts [23]. Detrended vegetation productivity indicators were used in the analysis (Figure 4). The response time is defined as the time elapsed from the onset of a flash drought to the first occurrence of a negative anomaly in vegetation productivity.

The recovery rate of vegetation productivity following a flash drought is defined as:

$$VPanomaly = \frac{VP-\mu_{VP}}{\sigma_{VP}} \quad (1)$$

where VP represents either GPP or SIF, and μ_{VP} and σ_{VP} denote the mean and standard deviation of the VP time series, respectively.

$$decreaserate = \frac{\overline{G_b}-G_a}{t_1} \quad (2)$$

where $G_a$is the minimum negative VP anomaly after a flash drought, $\overline{G_b}$ is the average of positive values in the three pentads before a flash drought, t_1 is the time length between $\overline{G_b}$ and G_a.

$$recoveryrate = \frac{G_e-G_a}{t_2} \quad (3)$$

where G_e is the first positive VP anomaly value occurring after G_a, and t_2 is the time interval between G_e and G_a.

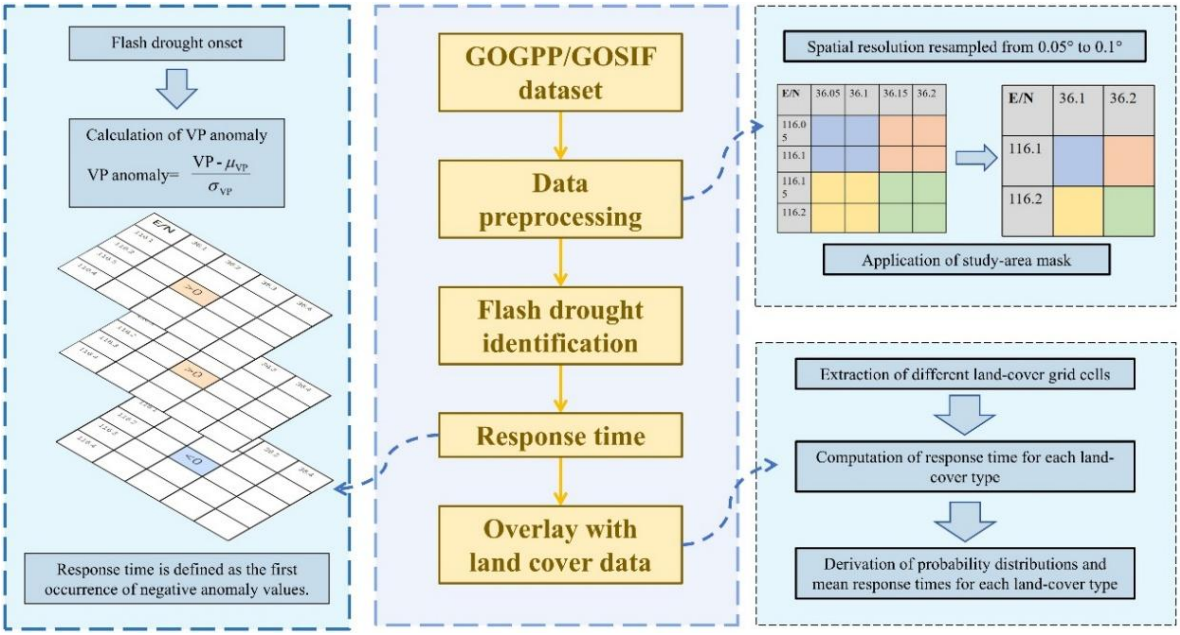

Figure 4. Workflow for SIF/GPP response analysis.

2.3.5. Random Forest and SHAP Interpretation Method

A Random Forest model was employed to identify the key driving factors influencing photosynthetic recovery rate (Figure 5). The Random Forest model exhibits robust nonlinear fitting capability and resistance to overfitting in ecological factor attribution analysis, and has been successfully applied to the analysis of global flash drought trend drivers, effectively quantifying the contributions of complex multi-factor interactions [46].

SHAP (Shapley Additive Explanations) values were adopted to quantify the average marginal contribution of each variable to the recovery rate and to rank the global importance of variables. The SHAP method possesses consistency and local interpretability, which effectively addresses the "black-box" limitations of conventional machine learning models [47] . This method has been

 doi:10.20944/preprints202605.1263.v1

successfully applied to disentangle the driving mechanisms of vegetation ecological processes, and can reveal the dominant mechanisms governing ecosystem recovery capacity across different regions. For instance, in the eastern monsoon region of China, SHAP analysis has confirmed that the contribution of flash drought duration to cropland photosynthetic recovery rate is 20%–30% higher than that of the temperature factor [48].

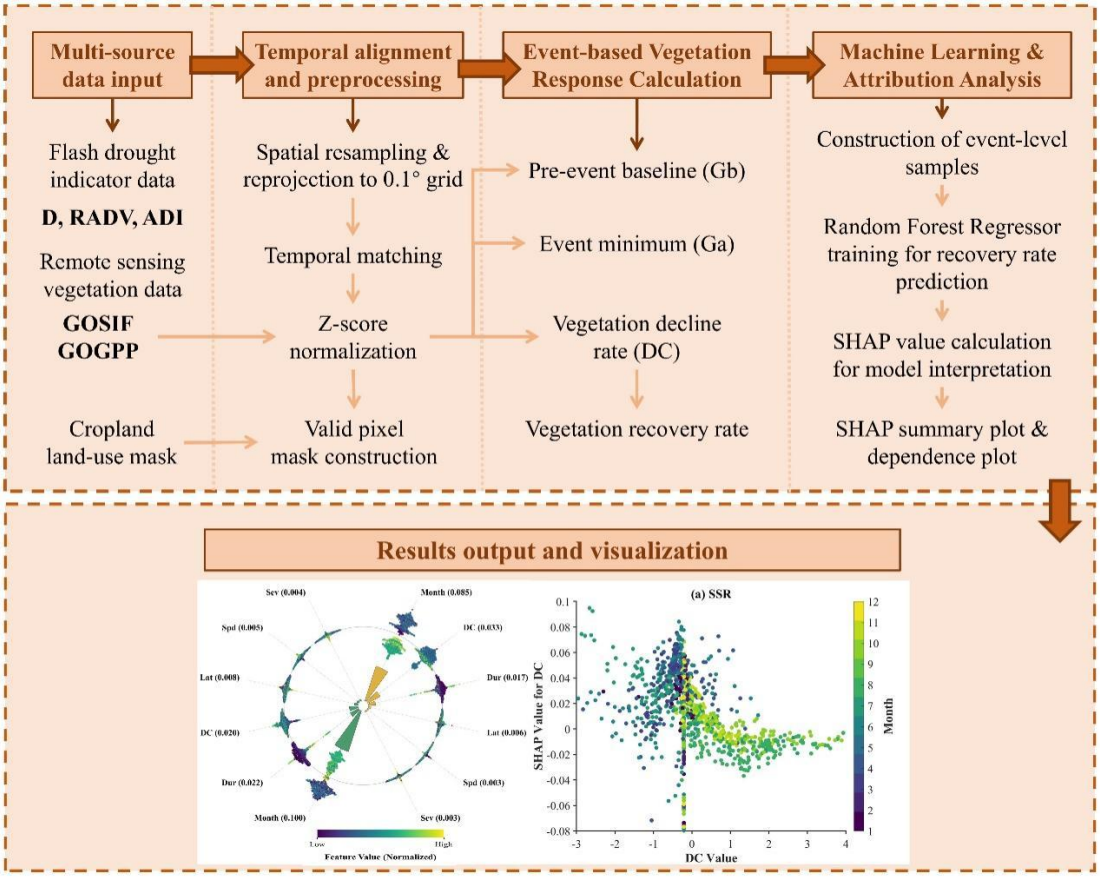

Figure 5. Flowchart of the random forest versus the SHAP interpretation method.

3. Results

3.1. Overall Characteristics of Flash Droughts Across the North China Plain and the Middle-Lower Yangtze Plain

Figure 6 illustrates the spatial distribution of flash drought characteristics across the two plains. In terms of total event count distribution, the high-incidence zones of flash drought are concentrated in the southern portion of the Middle-Lower Yangtze Plain, where the cumulative number of flash drought events reached approximately 20 over the period 2001–2024 (Figure 6a); by contrast, the southern North China Plain and the northern Middle-Lower Yangtze Plain exhibited relatively lower flash drought frequencies, with cumulative event counts of fewer than 5. Figures 6b and 6c present the flash drought duration and intensity, respectively. The central North China Plain exhibited the longest mean flash drought duration, reaching 10 or more octad (8-day) periods, accompanied by the highest mean intensity with severity indices predominantly around 300; in contrast, flash droughts in the southern Middle-Lower Yangtze Plain and the northern North China Plain were of shorter duration (4–6 octad periods) and weaker intensity (severity indices below 150). A pronounced north–south differentiation was observed in flash drought development speed (Figure 6d). The fastest flash drought development rates were observed in the northern North China Plain and the southern Middle-Lower Yangtze Plain (14–16%/8-day), indicating that droughts in these regions can escalate

 doi:10.20944/preprints202605.1263.v1

rapidly within a short period; whereas the development rates in the southern North China Plain and the northern Middle-Lower Yangtze Plain were comparatively moderate (8–10%/8-day).

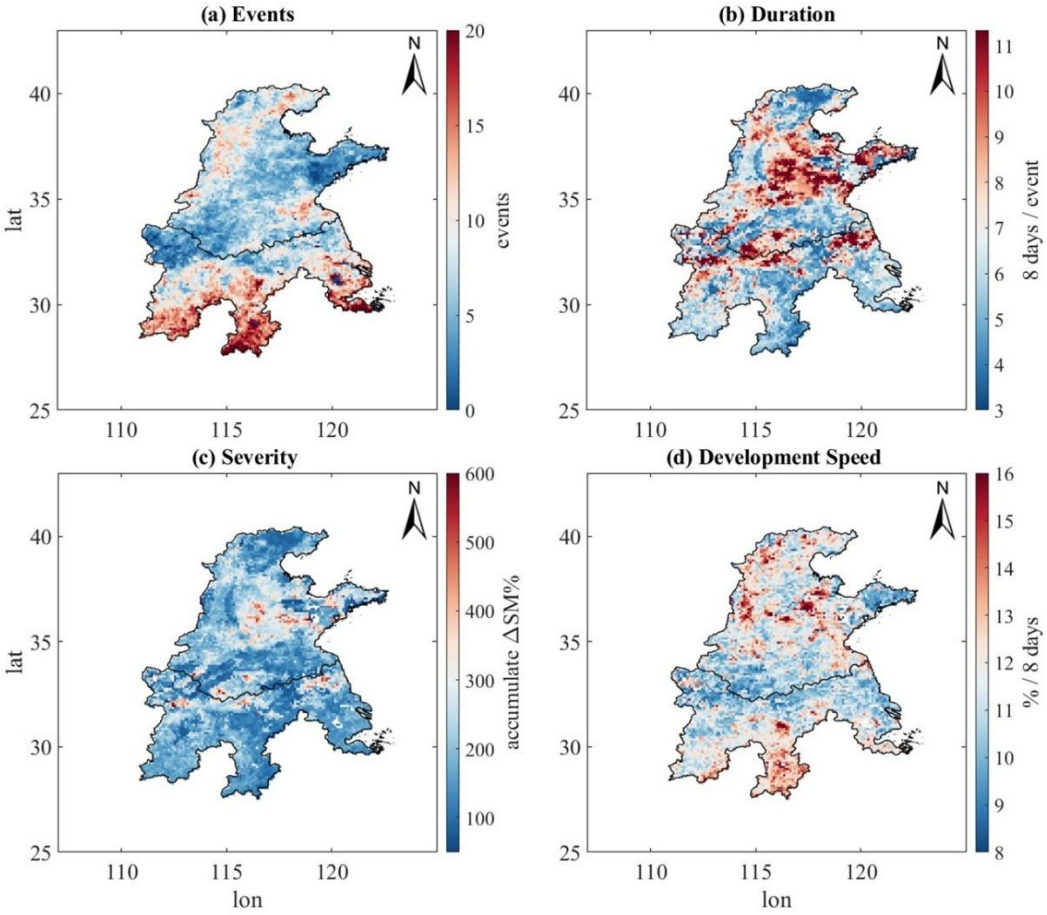

Figure 6. Spatial distribution of total number (a), average duration (b), average intensity (c) and average development rate (d) of sudden drought events in the study area from 2001 to 2024.

Significant differences were identified in the flash drought risk structure borne by different cropping systems (Figure 7). For rice systems (SSR/DSR), the frequency of flash drought encounters was markedly the highest, while the duration and severity were relatively low. This indicates that rice systems are subjected to flash droughts more frequently during their growing cycles, yet the intensity of individual events and cumulative deficit remain relatively limited, constituting a "high-frequency shock" type of risk. By contrast, although rainfed systems (WW/M) encountered flash droughts less frequently, their severity and duration were notably higher, suggesting that once a flash drought occurs, rainfed crops experience more prolonged and intense soil moisture depletion, with a more concentrated and acute risk of potential yield loss, constituting an "intensity-cumulative" type of risk. The risk profile of rotation systems (WW-SSR/WW-M) resembled that of rainfed systems, with lower event counts but higher severity and duration, reflecting that rotation systems are likewise sensitive to the cumulative effects of flash droughts. Notably, the flash drought development rates across all cropping systems were uniformly high (generally 10%–12%/8-day), indicating that "rapid intensification" is a core characteristic shared across different crops; however, the differences in frequency and intensity determine the type and consequences of the risk experienced by each crop. Overall, rice systems face high-frequency shock risks, whereas rainfed and rotation systems face intensity-cumulative risks, and this differentiation in risk structure carries important implications for agricultural disaster mitigation strategies.

 doi:10.20944/preprints202605.1263.v1

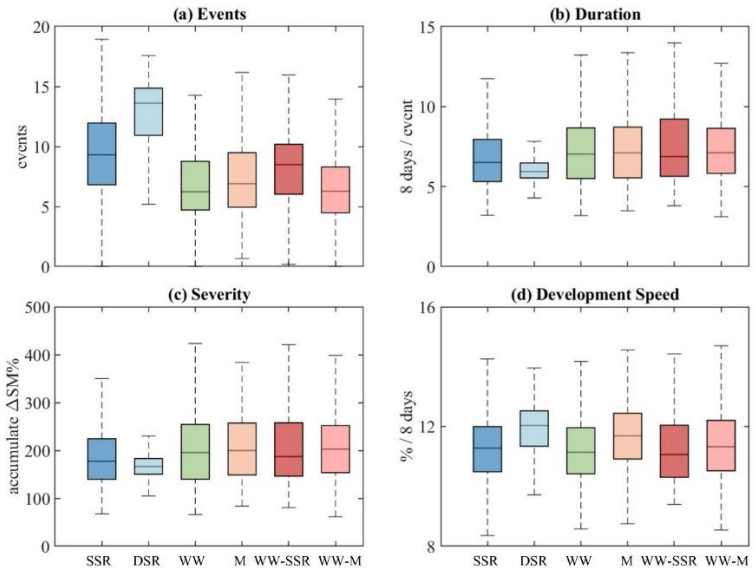

Figure 7. Boxplots of spatial distribution characteristics of flash droughts for different crops. Total number of flash drought events (a), average duration (b), average intensity (c) and average development rate (d).

3.2. Spatiotemporal Trajectory Characteristics of Flash Droughts

The interannual evolution of flash droughts in the study area over the period 2001–2024 was further analyzed. The results indicate (Figure S4) that the composite flash drought intensity indices for 2019 and 2022 were significantly higher than those of other years, marking these as the two representative severe years with the strongest intensity and longest duration during 2001–2024.

The flash drought centroids in 2019 (Figure 8(a)) and 2022 (Figure 8(b)) both exhibited pronounced dynamic migration characteristics, yet notable differences existed in the complexity of their migration paths and spatial evolution patterns. After initiating migration in mid-June 2019, the flash drought centroid followed a regular and coherent overall trajectory, with the spatial movement process characterized by smooth transitions and low path sinuosity, reflecting strong spatial continuity and directional stability in that year's flash drought development; from a temporal perspective, the centroid progression from mid-June to late December proceeded at a relatively uniform pace. In sharp contrast, the centroid migration trajectory in 2022 was considerably more complex, featuring multiple pronounced directional shifts and path reversals, with large spatial displacement amplitudes and conspicuous episodic leaping characteristics, highlighting the greater dynamism and instability of that year's spatiotemporal flash drought evolution.

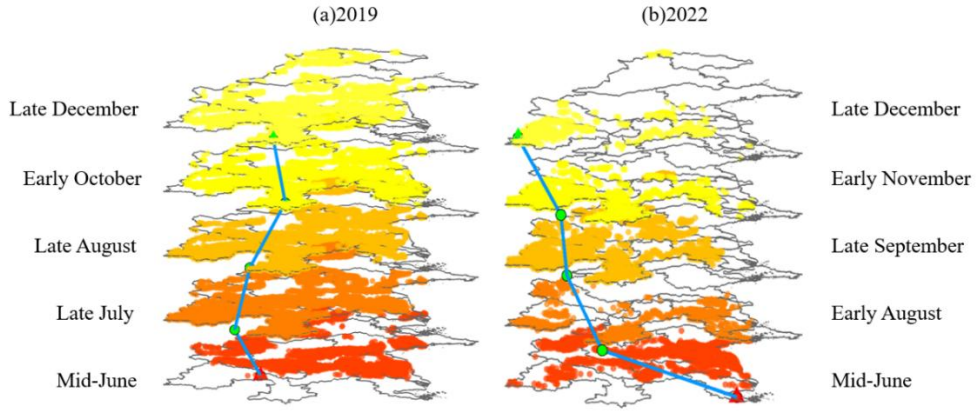

Trajectories of Spatiotemporal Centroid of Flash Drought in Typical Years (2019 and 2022)

 doi:10.20944/preprints202605.1263.v1

Figure 8. Trajectories of the spatiotemporal centroid of flash droughts in two typical years (2019 and 2022). The left and right panels show the movement paths for 2009 and 2019, respectively. Lines represent trajectories for different months, with green and red dots indicating the starting and ending points of each monthly centroid. The shaded areas highlight the trajectory regions.

3.3. Response Patterns of Vegetation Photosynthetic Indicators (SIF/GPP) to Flash Droughts

3.3.1. Overall Differences in SIF and GPP Response Times to Flash Droughts

As shown in Figure 9, the mean response time of SIF to flash droughts was consistently concentrated within the range of 16.0–17.4 days, while the mean response time of GPP was 22.0–25.2 days, with a systematic lag difference of approximately 6–9 days between the two (Figure 9). This difference was consistent across different crop types, indicating that SIF possesses an earlier physiological response capacity to flash droughts. The primary response peak of SIF was concentrated in the 8–18 day interval, with over 80% of events completing their response within 25 days; by comparison, the primary response peak of GPP was concentrated in the 16–32 day interval, with 80% of events typically completing their response around 30 days, and some crop types exhibiting delays exceeding 35 days.

From a spatial perspective, SIF response time exhibited an overall latitudinal gradient increasing from south to north. Response times in most areas of the Middle-Lower Yangtze Plain were concentrated at 5–15 days, those in the Huai River Basin at 10–20 days, and those in the central-northern North China Plain gradually increased to 15–25 days, locally exceeding 25 days. In contrast, the spatial heterogeneity of GPP response time was more pronounced: the Middle-Lower Yangtze Plain was dominated by 0–20 day responses, while the central-northern North China Plain generally exhibited 25–40 day responses, with some areas exceeding 40 days, manifesting a distinct lag amplification pattern.

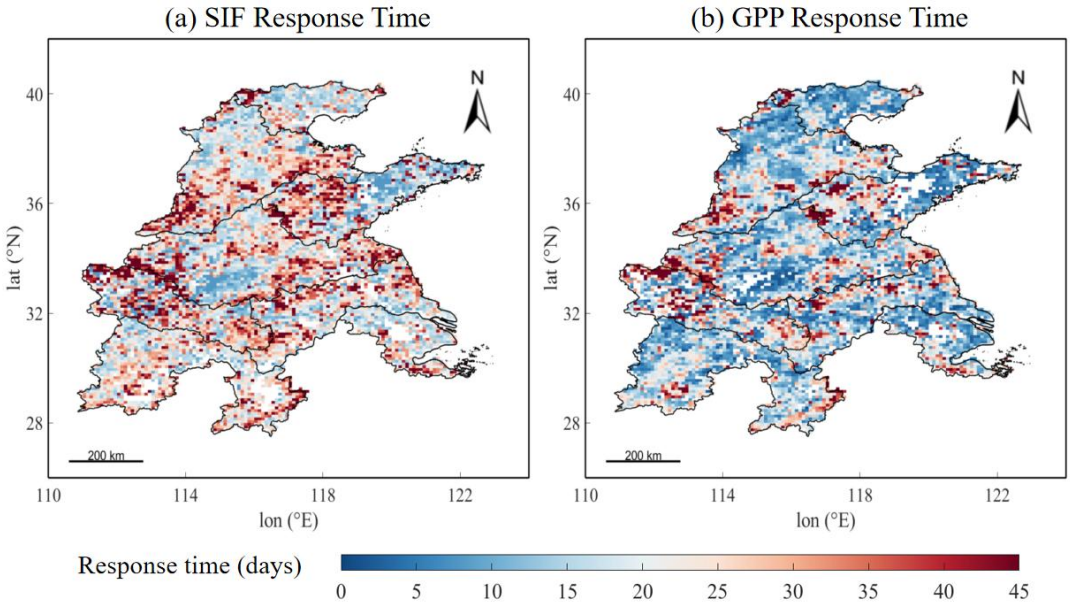

Figure 9. Average response time of GPP (a) and SIF (b) to flash droughts.

3.3.2. Differentiation in Photosynthetic Response Characteristics among Crop Types

As shown in Figure 10, the mean SIF response time across all crop types ranged from 16.0 to 17.4 days. SSR and M exhibited relatively faster responses (approximately 16.0–16.3 days), DSR and WW were slightly higher (approximately 16.5–17.0 days), and WW-SSR demonstrated the longest response time (approximately 17.4 days). The maximum inter-type difference was approximately 1–

 doi:10.20944/preprints202605.1263.v1

1.2 days, with an overall highly concentrated distribution, suggesting that the early physiological response captured by SIF possesses strong universality.

GPP response times were likewise concentrated within 22.0–25.2 days, though inter-type variation was slightly greater than that of SIF. Among these, WW-SSR exhibited the longest mean response time (approximately 25 days), M the shortest (approximately 22 days), with the remaining types predominantly distributed between 23 and 24 days. Despite minor variations, all crop types exhibited a consistent "SIF responds first, GPP responds later" structure.

Considering the regional cropping structure, the Middle-Lower Yangtze Plain is dominated by SSR and DSR, with flash drought responses characterized as the "rapid SIF response—relatively rapid GPP response" type; the North China Plain is dominated by WW-M and M, with an overall "moderate-speed SIF response—delayed GPP response" pattern. The GPP lag was most pronounced in WW-SSR regions.

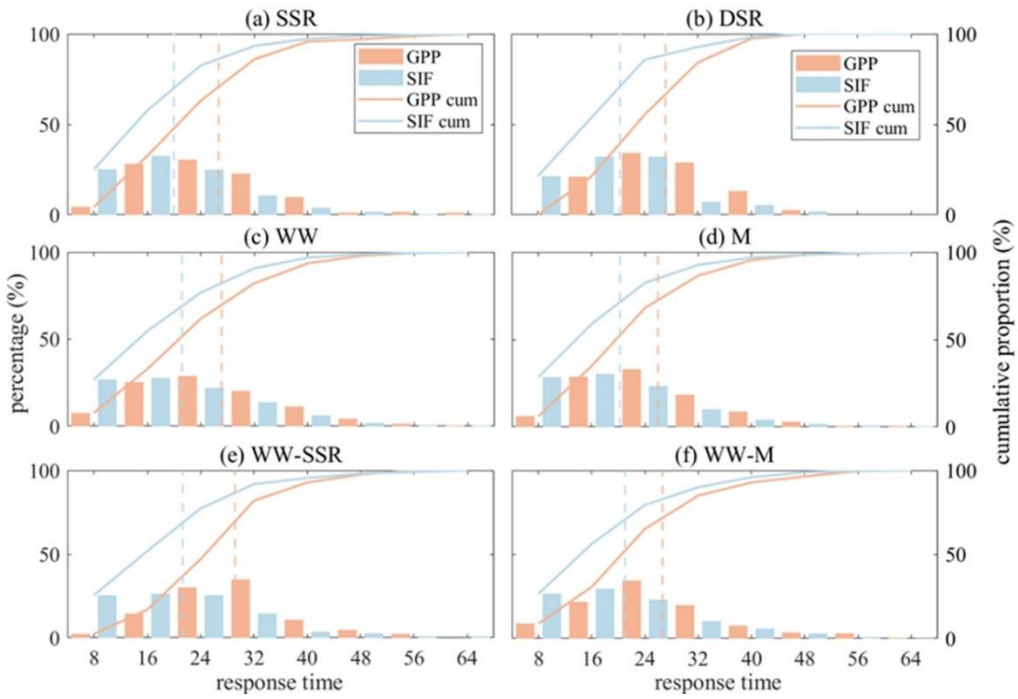

Figure 10. Mean and probability distribution of response time to flash droughts for different vegetation type.

3.4. SHAP Model-Based Analysis of Driving Factors for Crop Photosynthetic Recovery Rate

Building upon the differentiated response characteristics of crop photosynthetic indicators to flash droughts revealed in Section 3.3, SHAP values were further computed for each factor. As shown in Figure 11, the photosynthetic recovery of rice systems was strongly regulated by multiple flash drought characteristics (Figure 11(1, 2)). Beyond the dominant role of Month, the contributions of Duration and DC ranked closely behind. SHAP value analysis indicated that both longer Duration and faster DC were significantly associated with the suppression of photosynthetic recovery, revealing the intrinsic physiological characteristics of rice, namely its low tolerance and low adaptability to water supply interruptions. Notably, the SHAP value distributions of DSR across all features were generally broader than those of SSR, indicating that its photosynthetic recovery was more sensitive to changes in driving factors and that the system exhibited higher vulnerability.

Within rainfed systems, the photosynthetic recovery driving mechanisms of WW and M differed markedly (Figure 11(3, 4)). For WW, the absolute importance of the Month feature far exceeded that of all other factors, with the broadest SHAP value distribution, definitively anchoring the high risk of photosynthetic recovery suppression to specific phenological windows (e.g., spring). In comparison, the driving factor structure for M was more pluralistic, with DC and Sev serving as the

 doi:10.20944/preprints202605.1263.v1

key limiting factors second only to Month, indicating that rapidly intensifying moisture deficit poses a severe threat to its photosynthetic system.

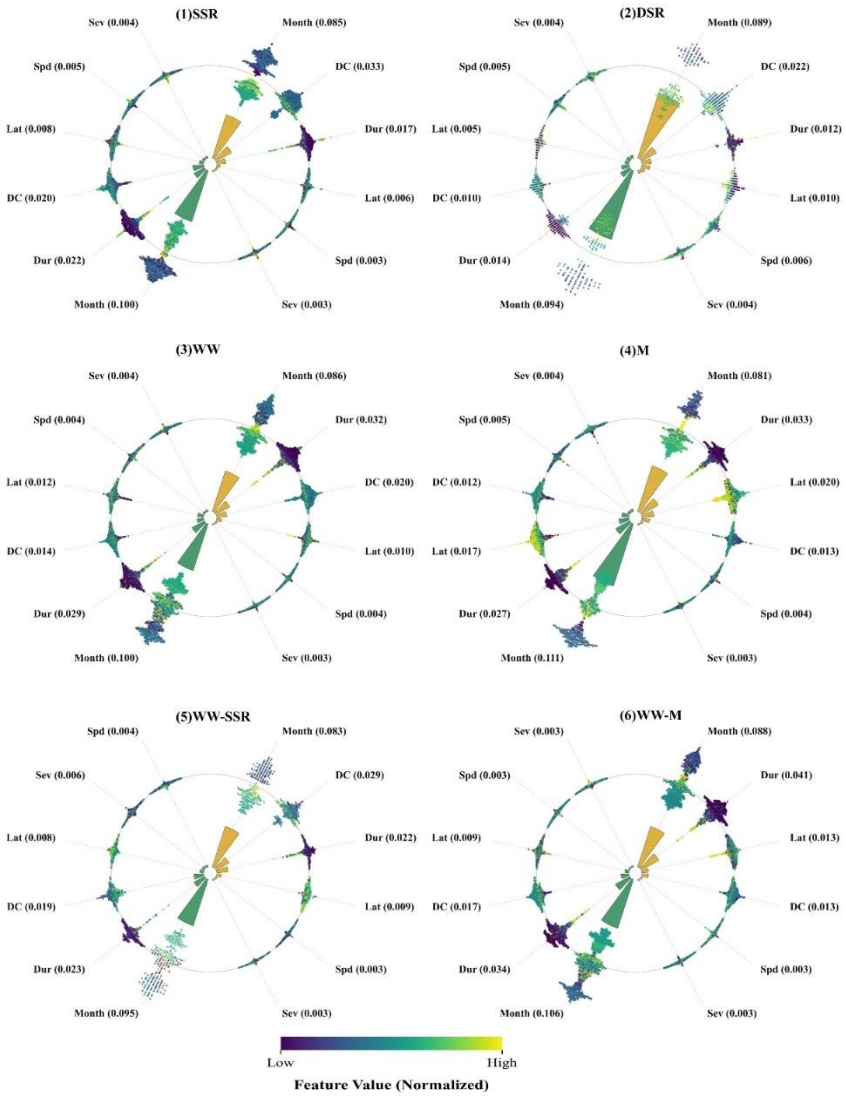

Figure 11. Polar SHAP integrated interpretation of drought drivers for SIF and GPP recovery. Note: The plot compares the importance and impact of drought characteristics on SIF (left) and GPP (right) recovery. Petal Length: Represents the mean absolute SHAP value, indicating global feature importance. Beeswarm Scatters: Each dot represents a sample; radial position indicates the SHAP value (contribution), and color indicates the feature value (Low to High). Variables: DC (decline rate), Dur (duration), Spd (development speed), Sev (severity), Lat (latitude), and Month.

Rotation systems integrate the physiological requirements of both preceding and succeeding crops, exhibiting more complex regulatory patterns (Figure 11(5, 6)). On one hand, Month remained the most important driving factor, yet its influence merged the phenologically sensitive periods of both crops. On the other hand, the importance of Duration was universally accentuated in rotation systems, reflecting the cumulative effects of cross-seasonal moisture stress. Of particular importance, compared to monoculture systems, the SHAP patterns of rotation systems revealed more balanced contributions among multiple process-related factors such as DC, Sev, and Spd, implying that their photosynthetic recovery is subject to multi-factor synergistic regulation and that the underlying mechanisms are more context-dependent.

To further elucidate the roles of key process-related factors, Figure 12 presents the SHAP dependence plots based on DC. The degree of photosynthetic recovery suppression intensified with

 doi:10.20944/preprints202605.1263.v1

increasing DC across all systems, though systematic differences in slope and dispersion were evident. Rice systems (particularly DSR) exhibited a larger negative shift in SHAP values at equivalent DC levels, accompanied by greater data point dispersion, corroborating their high sensitivity to rapid drought and the associated response uncertainty. The negative correlation trend line of M was the steepest, indicating that its photosynthetic recovery capacity declined precipitously with increasing DC. The scatter distributions of rotation systems exhibited greater dispersion than those of their corresponding monoculture counterparts, with intermingled coloring, supporting from an alternative perspective the complex regulation of their recovery processes by multi-factor interactions such as the "DC–timing of occurrence" interplay.

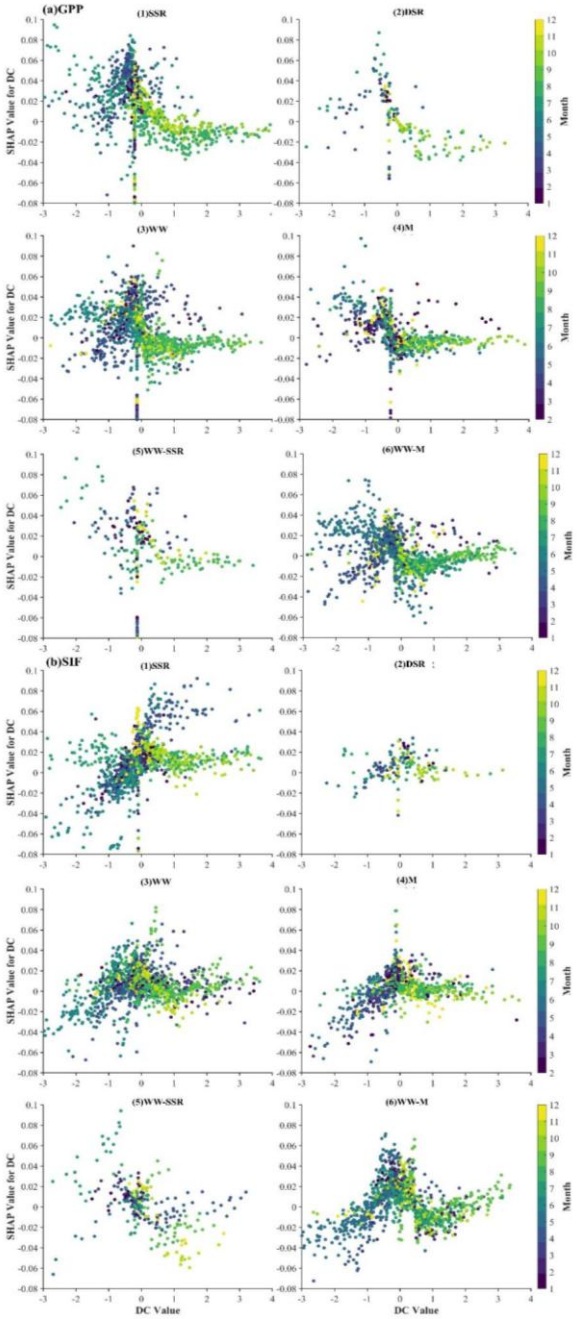

Figure 12. SHAP Values for Crop Photosynthesis against DC, Colored by Month. Note: This scatter plot illustrates the relationship between DC and SHAP values, with points colored by month (1-12, see color bar). The left and right columns correspond to the GPP and SIF photosynthetic indicators, respectively. Each row represents a different cropping system (SSR, DSR, WW, M, WW-SSR, WW-M). The horizontal axis denotes the

 doi:10.20944/preprints202605.1263.v1

DC value (representing the decline rate of vegetation productivity), and the vertical axis denotes the SHAP value (reflecting the magnitude of influence on recovery capacity).

4. Discussion

Through integrated multi-dataset, multi-method analysis, this study revealed the distinguishing characteristics of flash droughts in the North China Plain and the Middle-Lower Yangtze Plain and their manifestation across different cropping systems. The principal findings of this study are discussed in the following aspects:

4.1. Spatiotemporal Characteristics of Flash Droughts

In terms of overall flash drought characteristics, the southern Middle-Lower Yangtze Plain exhibited a "high-frequency—low-intensity" pattern, whereas the central North China Plain displayed a "low-frequency—high-intensity—long-duration" pattern, consistent with the "rapid intensification" characteristics of flash droughts proposed by Otkin et al. (2018). Development rates in most regions reached 8–16%/8-day, demonstrating that flash droughts in the East Asian monsoon region are equally characterized by abruptness and explosiveness. The causes of the aforementioned spatial heterogeneity may be attributed to regional differences in hydrothermal configurations and crop phenological stage sensitivity. On one hand, the North China Plain experiences high evapotranspiration demand and insufficient precipitation during spring [49], readily leading to persistent soil moisture deficits; on the other hand, although the Middle-Lower Yangtze Plain has relatively ample moisture conditions, it can rapidly transition to a high-temperature, low-precipitation regime under the dominance of the subtropical high-pressure system, thereby triggering short-duration flash droughts [50]. Furthermore, Yuan et al. noted that the enhanced atmospheric evaporative demand under global warming is accelerating flash drought occurrence [51], which resonates with the observed phenomenon of increasing development rates against the backdrop of north–south differentiation in this study.

The study further revealed significant differences in the flash drought risk borne by different crops: rice systems face "high-frequency shock" risks, with the highest event frequency but limited individual event intensity and cumulative deficit; whereas rainfed and rotation systems face "intensity-cumulative" risks, with fewer occurrences but markedly higher severity and duration. This finding deepens the understanding of flash drought impacts on agriculture.Shi et al.(2025), in their global-scale study of flash drought impacts on agricultural regions, noted that rainfed maize and wheat are primarily affected by droughts of moderate duration, whereas rainfed rice is more sensitive to short-duration droughts. This aligns with the inter-crop risk structure differences observed in the present study. The physiological mechanisms underlying the differential crop responses to flash droughts may be related to root depth and phenological stage. Previous studies have demonstrated that shallow-rooted vegetation is more sensitive to rapidly developing flash droughts [52]; rice systems possess relatively shallow root systems and respond rapidly to short-term moisture deficits but also recover quickly, thus manifesting a high-frequency, low-intensity pattern; whereas the critical reproductive growth stages (e.g., jointing to heading) experienced by rainfed and rotation systems are extremely sensitive to moisture stress, and once flash droughts occur, prolonged cumulative damage is readily incurred.

4.2. Differences in SIF–GPP Responses and Crop-Specific Divergence

The temporal difference (approximately 6–9 days) in SIF and GPP responses to flash droughts is, in essence, an external manifestation of the temporal decoupling between the light reactions and dark reactions of photosynthesis. SIF, serving as a probe of the actual photochemical efficiency of Photosystem II, can capture the signal of suppressed light energy utilization at the instant of stomatal conductance decline and VPD elevation [53]. In contrast, the carbon assimilation process (dark reactions) represented by GPP lies downstream of photosynthesis and is not only directly affected by

 doi:10.20944/preprints202605.1263.v1

stomatal limitation but also subject to cascading regulation by downstream processes including carboxylation efficiency, RuBP regeneration capacity, and metabolic substrate supply, resulting in a physiological lag in its response [54]. This interpretation is highly consistent with the flux observation-based conclusions of Mohammadi et al. (2022), who similarly found that SIF is capable of emitting drought stress signals 2–3 weeks before GPP decline [55] . The present study further refined the quantification of this temporal difference to 6–9 days and confirmed its stability across different cropping systems in the East Asian monsoon region, thereby further supporting the applicability of SIF as an early indicator of flash droughts.

This fundamental "rapid SIF response—slow GPP response" structure exhibited divergent characteristics across different cropping systems, reflecting the physiological differences in water stress adaptation strategies among cropping systems. In rice systems, SIF responded fastest and GPP lag was shortest, which is intimately related to their physiological architecture of shallow root systems and high stomatal conductance: stomata close rapidly to prevent water loss, but simultaneously lead to reduced light energy utilization efficiency and impaired carbon assimilation [56]. This resonates with the observations of Yang et al. (2024) in paddy ecosystems—that the physiological response of rice to atmospheric drought is extremely rapid, yet the recovery of photosynthetic capacity is also relatively swift. By contrast, the pronounced GPP delay in rainfed systems may signify the involvement of non-stomatal limitation factors [54]. Li et al. (2023) noted that C4 crops such as maize can sustain their carbon assimilation rates for a period through osmotic adjustment and mobilization of carbon reserves under drought stress, thereby delaying the substantive decline in GPP. Although this physiological buffering capacity masks losses in the short term, it may also lead decision-makers to misjudge the severity of drought.

The response characteristics of rotation systems highlight the role of temporal configuration in cropping system design. The winter wheat–single-season rice rotation (WW-SSR) exhibited the longest SIF response time and the most pronounced GPP lag, revealing the amplifying effect of the crop transition period on moisture stress: during the fallow interval between winter wheat harvest and single-season rice transplanting (approximately 15–30 days), the land surface lacks vegetation cover, and soil moisture is substantially lost through evaporation, placing the system in a state of fragile equilibrium [57]. If flash drought strikes at this juncture, the root system of the succeeding rice crop at the time of transplanting has yet to be fully developed, its capacity to sense soil moisture deficit is weak, and ABA signal transduction efficiency is low, preventing the timely activation of physiological response mechanisms, which is manifested as a significantly delayed SIF response time [58]. By the time roots become gradually established and capable of perceiving the stress, soil moisture has already been severely depleted, and the crop has entered an irreversible phase of damage. In contrast, the winter wheat–maize rotation (WW-M), also a rotation system, did not exhibit a significant response delay, owing to the high continuity of its crop transition—summer maize is immediately relay-planted following winter wheat harvest with virtually no bare-soil period, establishing an effective relay in soil moisture utilization that mitigates the impact of moisture stress. This comparison reveals that the vulnerability of cropping systems depends not only on the inherent physiological attributes of the crops themselves but also critically on the temporal configuration of the cropping system.

4.3. Recovery Driving Mechanisms Revealed by the SHAP Model

Based on the SHAP interpretable model, this study quantitatively revealed the driving mechanisms by which flash droughts affect crop photosynthetic recovery, highlighting the critical dominant role of phenological stage in agricultural flash drought assessment and elucidating the hierarchical nature and system specificity of driving factors. This conclusion is highly consistent with the global-scale study by Shi et al. (2025), which confirmed that the regulatory role of phenological stage on flash drought damage is significantly higher than that of traditional indices such as intensity and duration, and proposed a hierarchical framework of phenological stage > drought process

 doi:10.20944/preprints202605.1263.v1

characteristics > agricultural management [59], jointly corroborating the central position of phenological timing in agricultural flash drought impact assessment.

This study found that the contribution weight of the month of drought occurrence to photosynthetic recovery exceeded those of Sev and Duration (Figure 14), providing supplementary insights to conventional drought research [60]. Annual crops possess strictly irreversible phenological progressions, and the coupling of stress periods with physiologically vulnerable windows serves as a key amplifier of impact magnitude. A moderate flash drought occurring during the critical reproductive stage (heading to grain filling) impedes the photosynthetic system and yield to a far greater extent than a high-intensity drought occurring in the late vegetative stage. This result supports the high temporal heterogeneity of vegetation drought responses proposed by Li et al. (2023), and provides a basis for the quantification and weighting of "phenological windows" in regional cropping systems.

Under the dominance of phenological timing, flash drought development rate and duration jointly modulate the degree of damage. This study demonstrated that DC is of greater importance than Sev, consistent with the proposition by Otkin et al. (2018) that rapid onset constitutes the core hazard-inducing property of flash droughts. Rapid development compresses the windows for crop physiological adjustment and management intervention, triggering instantaneous responses such as stomatal closure and Photosystem II damage; sustained stress depletes available soil water, leading to osmotic regulation imbalance, carbon reserve exhaustion, and diminished recovery potential. The extraordinary flash drought in the Yangtze River Basin in 2022 corroborated the aforementioned cumulative effects and positive feedback mechanisms [61]. The dual high sensitivity of rice to both DC and Duration originates from the inherent contradiction between its high root oxygen demand and high transpiration requirements, which are legacies of its aquatic adaptation.

The response differences among different cropping systems originate from their distinct physiological characteristics and management practices. Due to its well-developed aerenchyma, high root oxygen demand, and adaptation to prolonged waterlogged conditions, rice suffers significant root and photosynthetic system damage upon water withdrawal [62]; double-season rice, with its compact growth cycle and insufficient recovery redundancy, exhibits even higher sensitivity [63]. Winter wheat is extremely sensitive to spring drought, stemming from the irreversible physiological investment during the vernalization-to-reproductive transition, with stress readily causing floret degeneration and weak resilience. Maize, as a C4 crop, pairs high photosynthetic efficiency with high transpiration, rendering it particularly vulnerable to rapidly developing droughts (high DC). Rotation systems have low tolerance to sustained drought, as the preceding crop depletes deep soil water, elevating the moisture deficit baseline for the succeeding crop, while overlapping phenological windows extend the risk exposure period [64].

4.5. Limitations and Future Perspectives

This study conducted a systematic analysis of flash drought characteristics and crop response mechanisms across the North China Plain and the Middle-Lower Yangtze Plain; however, three aspects of limitations remain. First, although the multi-source soil moisture data underwent error assessment via the Triple Collocation method, the SMCI1.0 time series extends only to 2022, and minor discrepancies persist between reanalysis datasets and in-situ observations, which to some extent affect the level of refinement in flash drought identification. Second, the study did not incorporate anthropogenic agricultural activity factors such as irrigation, fertilization, and cultivar breeding, yet given that the study area constitutes China's core grain-producing region where human intervention significantly regulates crop flash drought response and recovery, a complete elucidation of flash drought ecological effects under natural–anthropogenic coupling remains challenging. Third, only the historical characteristics and impacts of flash droughts during 2001–2024 were analyzed, without integrating climate model projections for future scenario-based flash drought evolution prediction, thus lacking a forward-looking analysis of flash drought risk under climate change.

 doi:10.20944/preprints202605.1263.v1

Future research may pursue in-depth investigation along three directions: first, integrating multi-station in-situ soil moisture observations from the study area to optimize multi-source soil moisture data fusion methods and enhance the accuracy and resolution of flash drought identification and spatiotemporal trajectory characterization; second, establishing a natural–anthropogenic coupled analytical framework that incorporates human activity indicators such as irrigation intensity and cropping system adjustments to quantify the synergistic contributions and interactions of natural and anthropogenic factors on flash drought formation and crop response; and third, combining CMIP6 and other climate model outputs to simulate the spatiotemporal evolution trends of flash droughts under different carbon emission scenarios, to reveal the potential impacts of future flash droughts on photosynthesis and yield of major crops, and to propose targeted adaptation strategies.

5. Conclusions

This study investigated the spatiotemporal characteristics of flash droughts in the North China Plain and the Middle-Lower Yangtze Plain of China and their impacts on crop photosynthetic recovery. The principal conclusions are as follows: flash drought events exhibited pronounced regional differences in frequency, duration, and development rate, with the southern Middle-Lower Yangtze Plain and the central North China Plain characterized by high frequency and high intensity versus prolonged duration, respectively; SIF signals and GPP data demonstrated that different cropping systems exhibit temporal differences in their response mechanisms to flash droughts, presenting a "rapid SIF response—lagged GPP recovery" pattern that offers a new perspective for proactive early warning; the multi-data source fusion and Random Forest model employed in this study provided quantitative analysis of driving factors, preliminarily revealing the key variables in the drought progression, although data limitations and regional representativeness issues require further refinement in future research; moreover, this study contributes to deepening the understanding of rapid drought response mechanisms while providing scientific reference for regional agricultural disaster prevention and food security management. In summary, this study conducted a relatively systematic analysis of flash drought events based on multi-source data and analytical methods, and delineated clear directions for future research. Future in-depth investigations hold the promise of further enhancing the sensitivity and accuracy of regional drought early warning systems, thereby better serving agricultural production and ecological environmental protection.

Supplementary Materials: The following supporting information can be downloaded at the website of this paper posted on Preprints.org.

Author Contributions: Shuo Mao: Methodology, Writing—original draft. **Mengzhen Han**: Methodology, Writing—original draft, Validation. **Hao Chen**: Methodology, Writing—original draft. **Shaowei Ning:** Conceptualization, Supervision, Writing—review & editing. **Zhenyu Zhang**: Writing—review & editing, Validation. **Le Chen:** Visualization, Software. **Yuliang Zhou:** Resources, Funding acquisition. **Weimin Ju**: Data curation, Formal analysis.

Funding: This work was supported by the National Training Program of Innovation and Entrepreneurship for Undergraduates (grant number: S202510359408), National Natural Science Foundation of China (Grant nos. 52379006; 32501471).

Data Availability Statement: Data will be made available on request.

Acknowledgments: The authors appreciated the editor and anonymous reviewers for their constructive comments and suggestions on the revision of this paper.

Conflicts of Interest: The authors declare that they have no known competing financial interests or personal relationships that could have appeared to influence the work reported in this paper.

 doi:10.20944/preprints202605.1263.v1

Abbreviations

The following abbreviations are used in this manuscript:

FD	Flash drought
RZSM	Root zone soil moisture
SSR	Single-season rice
DSR	Double-season rice
WW	Winter wheat
M	Maize
WW-M	Winter wheat-maize
WW-SSR	Winter wheat-single-season rice
TC	Triple Collocation
EDF	Empirical Distribution Function
SHAP	Shapley Additive Explanations
GOSIF	Global dataset of solar-induced chlorophyll fluorescence
GPP	Gross primary production
ECMWF	European Centre for Medium-Range Weather Forecasts
GLEAM	Global Land Evaporation Amsterdam Model
SMCI1.0	Soil Moisture of China by in situ data, version 1.0
CCD	China Crop Dataset

References

1. Goswami P., & Gallant. A.J.. (2025). Understanding Drought Onset: What Makes Flash Droughts Different From Conventional Droughts?. Weather and Climate Extremes, 49(null), null. https://link.cnki.net/doi/10.1016/J.WACE.2025.100782. 10.1016/J.WACE.2025.100782.
2. Qing Y., Wang S., Ancell B.C., & Yang Z.. (2022). Accelerating Flash Droughts Induced By the Joint Influence of Soil Moisture Depletion and Atmospheric Aridity. Nature Communications, 13. https://doi.org/10.1038/s41467-022-28752-4. 10.1038/s41467-022-28752-4.
3. Yuan X., Wang Y., Ji P., Wu P., Sheffield J., & Otkin J.A.. (2023). A Global Transition to Flash Droughts Under Climate Change. Science, 380, 187-191. https://doi.org/10.1126/science.abn6301. 10.1126/science.abn6301.
4. Gu L., Schumacher D.L., Fischer E.M., Slater L.J., Yin J., Sippel S., Chen J., Liu P., & Knutti R.. (2025). Flash Drought Impacts on Global Ecosystems Amplified By Extreme Heat. Nature Geoscience, 18, 709-715. https://doi.org/10.1038/s41561-025-01719-y. 10.1038/s41561-025-01719-y.
5. A. L.M., Josefina P.M., V. M.O., V. M.G., & H.. B.E.. (2024). The Prevalent Life Cycle of Agricultural Flash Droughts. Npj Climate and Atmospheric Science, 7(1), null. https://link.cnki.net/doi/10.1038/S41612-024-00618-0. 10.1038/S41612-024-00618-0.
6. Wang Y., & Yuan X.. (2022). Land-atmosphere Coupling Speeds Up Flash Drought Onset. Science of the Total Environment, 851, 158109. https://doi.org/10.1016/j.scitotenv.2022.158109. 10.1016/j.scitotenv.2022.158109.
7. Walker C., Ellenburg W.L., Mishra V., Mecikalski J.R., Hain C.R., & Anderson M.C.. (2026). Evaporative Stress Index as a Flash Drought Tool in the Southeastern U.s.. Journal of Hydrology: Regional Studies, 64, 103245. https://doi.org/10.1016/j.ejrh.2026.103245. 10.1016/j.ejrh.2026.103245.
8. Zhu Y., Yang P., Xia J., Huang H., Chen Y., Li L., Sun K., Song J., Shi X., & Lu X.. (2025). Differential Impact of Flash Droughts on Water Use Efficiency in Terrestrial Ecosystems in Central Asia. Climatic Change, 178. https://doi.org/10.1007/s10584-025-03894-8. 10.1007/s10584-025-03894-8.
9. Nguyen N.M., Lee S., & Kim J.. (2026). Evaluating the Applicability of Exclusively Optical Sensors in Flash Drought Monitoring with Modis Observations. Isprs Journal of Photogrammetry and Remote Sensing, 231, 376-393. https://doi.org/10.1016/j.isprsjprs.2025.10.031. 10.1016/j.isprsjprs.2025.10.031.
10. Qi Z., Ye Y., Sun L., Yuan C., Cai Y., Xie Y., Cheng G., & Zhang P.. (2025). Development of an Indicator System for Solar-induced Chlorophyll Fluorescence Monitoring to Enhance Early Warning of Flash Drought. Agricultural Water Management, 312, 109397. https://doi.org/10.1016/j.agwat.2025.109397. 10.1016/j.agwat.2025.109397.

 doi:10.20944/preprints202605.1263.v1

11. Saharwardi M.S., Hassan W.U., Dasari H.P., Abualnaja Y., & Hoteit I.. (2025). Enhanced Flash Droughts in Recent Decades Over the Arabian Peninsula. *Journal of Hydrology: Regional Studies, 61*, 102696. https://doi.org/10.1016/j.ejrh.2025.102696. 10.1016/j.ejrh.2025.102696.
12. Harris B.L., Taylor C.M., Dorigo W., Zotta R., Ghent D., & Noguera I.. (2025). Global Observations of Land-atmosphere Interactions During Flash Drought. Hydrology and Earth System Sciences, 29, 6917-6933. https://doi.org/10.5194/hess-29-6917-2025. 10.5194/hess-29-6917-2025.
13. Yin G., He W., Liu W., Liu X., Xia Y., & Zhang H.. (2024). Drought Stress and Its Characteristics in China From 2001 to 2020 Considering Vegetation Response and Drought Creep Effect. Journal of Hydrology: Regional Studies, 53, 101763. https://doi.org/10.1016/j.ejrh.2024.101763. 10.1016/j.ejrh.2024.101763.
14. Zhou Z., Wang P., Li L., Fu Q., Ding Y., Chen P., Xue P., Wang T., & Shi H.. (2024). Recent Development on Drought Propagation: a Comprehensive Review. Journal of Hydrology, 645, 132196. https://doi.org/10.1016/j.jhydrol.2024.132196. 10.1016/j.jhydrol.2024.132196.
15. Shadmehri toosi A., Batelaan O., Shanafield M., & Guan H.. (2025). Land Use-land Cover and Hydrological Modeling: a Review. Wires Water, 12. https://doi.org/10.1002/wat2.70013. 10.1002/wat2.70013.
16. Wang, Wenliang, Zhou, Lei, He, Congcong, Zhang, Yongwen, Gong, Zhiqiang, Ying, Na, Qiao, Panjie, Wu, Jianjun, Sun, Hongquan, Fan, & Jingfang. (2025). Complex Network Approaches for Identifying Global Drought Teleconnection Patterns. Global and Planetary Change, 105093.
17. Dai S., Zhang Q., & Huang S.. (2025). Identification and Characteristics of Regional Rainstorm Events in China Based on a Dual-threshold Method. Atmospheric Research, 320, 108081. https://doi.org/10.1016/j.atmosres.2025.108081. 10.1016/j.atmosres.2025.108081.
18. Li J., Chen L., Zhang G., Liu H., Hu H., Xu M., Guo X., Meng Z., & Dong Z.. (2025). Identification and Characterization of Long-term Meteorological Drought Events in the Yellow River Basin. Ecological Informatics, 86, 102992. https://doi.org/10.1016/j.ecoinf.2025.102992. 10.1016/j.ecoinf.2025.102992.
19. Huang C., Huang J., Xiao J., Li X., He H.S., Liang Y., Chen F., & Tian H.. (2024). Global Convergence in Terrestrial Gross Primary Production Response to Atmospheric Vapor Pressure Deficit. Science China Life Sciences, 67, 2016-2025. https://doi.org/10.1007/s11427-023-2475-9. 10.1007/s11427-023-2475-9.
20. Zhao Y., Xiong L., Yin J., Zha X., Li W., & Han Y.. (2024). Understanding the Effects of Flash Drought on Vegetation Photosynthesis and Potential Drivers Over China. Science of the Total Environment, 931, 172926. https://doi.org/10.1016/j.scitotenv.2024.172926. 10.1016/j.scitotenv.2024.172926.
21. Meng F., Liu D., Wang Y., Wang S., & Wang T.. (2023). Negative Relationship Between Photosynthesis and Late-stage Canopy Development and Senescence Over Tibetan Plateau. Global Change Biology, 29, 3147-3158. https://doi.org/10.1111/gcb.16668. 10.1111/gcb.16668.
22. O S., Park S.K.. (2023). Flash Drought Drives Rapid Vegetation Stress in Arid Regions in Europe. Environmental Research Letters, 18, 014028. https://doi.org/10.1088/1748-9326/acae3a. 10.1088/1748-9326/acae3a.
23. Yang L., Wang W., & Wei J.. (2023). Assessing the Response of Vegetation Photosynthesis to Flash Drought Events Based on a New Identification Framework. Agricultural and Forest Meteorology, 339, 109545. https://doi.org/10.1016/j.agrformet.2023.109545. 10.1016/j.agrformet.2023.109545.
24. Wang X., Blanken P.D., Wood J.D., Nouvellon Y., Thaler P., Kasemsap P., Chidthaisong A., Petchprayoon P., Chayawat C., Xiao J., & Li X.. (2023). Solar-induced Chlorophyll Fluorescence Detects Photosynthesis Variations and Drought Effects in Tropical Rubber Plantation and Natural Deciduous Forests. Agricultural and Forest Meteorology, 339, 109591. https://doi.org/10.1016/j.agrformet.2023.109591. 10.1016/j.agrformet.2023.109591.
25. Wang H., Zhu Q., Wang Y., & Zhang H.. (2023). Spatio-temporal Characteristics and Driving Factors of Flash Drought Recovery: From the Perspective of Soil Moisture and Gpp Changes. Weather and Climate Extremes, 42, 100605. https://doi.org/10.1016/j.wace.2023.100605. 10.1016/j.wace.2023.100605.
26. Zeng Z., Wu W., Li Y., Huang C., Zhang X., Peñuelas J., Zhang Y., Gentine P., Li Z., Wang X., Huang H., Ren X., & Ge Q.. (2023). Increasing Meteorological Drought Under Climate Change Reduces Terrestrial Ecosystem Productivity and Carbon Storage. One Earth, 6, 1326-1339. https://doi.org/10.1016/j.oneear.2023.09.007. 10.1016/j.oneear.2023.09.007.

 doi:10.20944/preprints202605.1263.v1

27. Mohammadi, Koushan, Jiang, Yelin, Wang, & Guiling. (2022). Flash Drought Early Warning Based on the Trajectory of Solar-induced Chlorophyll Fluorescence. *Proceedings of the National Academy of Sciences, 119*(32), e2202767119
28. Sun J., Zhang Q., Liu X., Sun J., Chen L., Wu Y., Hu B., & Zhang G.. (2024). Flash Droughts in a Hotspot Region: Spatiotemporal Patterns, Possible Climatic Drivings and Ecological Impacts. Weather and Climate Extremes, 45, 100700. https://doi.org/10.1016/j.wace.2024.100700. 10.1016/j.wace.2024.100700.
29. Yang L., Wang W., & Wei J.. (2023). Assessing the Response of Vegetation Photosynthesis to Flash Drought Events Based on a New Identification Framework. Agricultural and Forest Meteorology, 339, 109545. https://doi.org/10.1016/j.agrformet.2023.109545. 10.1016/j.agrformet.2023.109545.
30. Xiao C., Zaehle S., Yang H., Wigneron J., Schmullius C., & Bastos A.. (2023). Land Cover and Management Effects on Ecosystem Resistance to Drought Stress. Earth System Dynamics, 14, 1211-1237. https://doi.org/10.5194/esd-14-1211-2023. 10.5194/esd-14-1211-2023.
31. Zhang M., Yuan X., Zeng Z., Pan M., Wu P., Xiao J., & Keenan T.F.. (2025). A Pronounced Decline in Northern Vegetation Resistance to Flash Droughts From 2001 to 2022. Nature Communications, 16. https://doi.org/10.1038/s41467-025-58253-z. 10.1038/s41467-025-58253-z.
32. Shi R., Liu Y., Zhu Y., Ren L., Liu Y., Zhang X., & Zhang L.. (2025). Impact of Flash Droughts on Global Crop Yields Considering Crop Phenology and Irrigation Conditions. Agricultural and Forest Meteorology, 373, 110763. https://doi.org/10.1016/j.agrformet.2025.110763. 10.1016/j.agrformet.2025.110763.
33. Orth R., Destouni G., Jung M., & Reichstein M.. (2020). Large-scale Biospheric Drought Response Intensifies Linearly with Drought Duration in Arid Regions. Biogeosciences, 17, 2647-2656. https://doi.org/10.5194/bg-17-2647-2020. 10.5194/bg-17-2647-2020.
34. Wang Y., Fu Z., Hu Z., & Niu S.. (2022). Tracking Global Patterns of Drought-induced Productivity Loss Along Severity Gradient. Journal of Geophysical Research: Biogeosciences, 127. https://doi.org/10.1029/2021jg006753. 10.1029/2021jg006753.
35. Yin J., Gentine P., Slater L., Gu L., Pokhrel Y., Hanasaki N., Guo S., Xiong L., & Schlenker W.. (2023). Future Socio-ecosystem Productivity Threatened By Compound Drought–heatwave Events. Nature Sustainability, 6, 259-272. https://doi.org/10.1038/s41893-022-01024-1. 10.1038/s41893-022-01024-1.
36. Yuan, Xing, Wang, Linying, Wu, Peili, Ji, Peng, Sheffield, Justin, Zhang, & Miao. (2019). Anthropogenic Shift Towards Higher Risk of Flash Drought Over China. Nature Communications, 10(1), 4661.
37.
1. Kim H., Crow W., Li X., Wagner W., Hahn S., & Lakshmi V.. (2023). True Global Error Maps for Smap, Smos, and Ascat Soil Moisture Data Based on Machine Learning and Triple Collocation Analysis. Remote Sensing of Environment, 298, 113776. https://doi.org/10.1016/j.rse.2023.113776. 10.1016/j.rse.2023.113776.
38. Sun J., Zhang Q., Liu X., Sun J., Chen L., Wu Y., Hu B., & Zhang G.. (2024). Flash Droughts in a Hotspot Region: Spatiotemporal Patterns, Possible Climatic Drivings and Ecological Impacts. Weather and Climate Extremes, 45, 100700. https://doi.org/10.1016/j.wace.2024.100700. 10.1016/j.wace.2024.100700.
39. Qi, Zixuan, Ye, Yuchen, Sun, Lian, Yuan, Chaoxia, Cai, Yanpeng, Xie, Yulei, Cheng, Guanhui, Zhang, & Pingping. (2025). Development of an Indicator System for Solar-induced Chlorophyll Fluorescence Monitoring to Enhance Early Warning of Flash Drought. Agricultural Water Management, 312, 109397.
40. Mccoll K.A., Vogelzang J., Konings A.G., Entekhabi D., Piles M., & Stoffelen A.. (2014). Extended Triple Collocation: Estimating Errors and Correlation Coefficients with Respect to an Unknown Target. Geophysical Research Letters, 41, 6229-6236. https://doi.org/10.1002/2014gl061322. 10.1002/2014gl061322.
41. Otkin, A J., Svoboda, Mark, Hunt, D E., Ford, W T., Anderson, C M., Hain, Christopher, Basara, & B J.. (2018). Flash Droughts: a Review and Assessment of the Challenges Imposed By Rapid-onset Droughts in the United States. Bulletin of the American Meteorological Society, 99(5), 911-919.
42. Resources S.O.H.A.W., Technology N.U.O.I.S.A., Nanjing, 210044, Jiangsu, Xyuan@nuist.edu.cn. C., (rce-tea) K.L.O.R.C.F.T.E.A., Physics I.O.A., Sciences C.A.O., Beijing, 100029, Xyuan@nuist.edu.cn. C., (rce-tea) K.L.O.R.C.F.T.E.A., Physics I.O.A., Sciences C.A.O., Beijing, 100029, China., Centre M.O.H. ... China... (2019). Anthropogenic Shift Towards Higher Risk of Flash Drought Over China. Nature Communications, 10(1), null. https://link.cnki.net/doi/10.1038/s41467-019-12692-7. 10.1038/s41467-019-12692-7.

 doi:10.20944/preprints202605.1263.v1

43. Schmoldt A., Benthe H.F., Haberland G., Fänge R., Johansson-sjöbeck M.L., Barthel W., Markwardt F., Dicker K.A., Löwenberg B., Schaefer U.W., Van bekkum D.W., Makar A.B., Mcmartin K.E., Palese M., & Tephly T.R.. (1975). Digitoxin Metabolism By Rat Liver Microsomes.. Biochemical Pharmacology, 24(17), 1639-1641.
44. Leeper, D R., Petersen, Bryan, Palecki, A M., Diamond, & Howard. (2021). Exploring the Use of Standardized Soil Moisture as a Drought Indicator. Journal of Applied Meteorology and Climatology, 60(8), 1021-1033.
45. Wang, Dingkui, Tan, Xuezhi, Wu, Xinxin, Huang, Zeqin, Deng, Simin, Liu, Yaxin, Fu, Jianyu, Tan, Xuejin, Cai, Xitian, Liu, & Bingjun. (2025). Dynamic Development of Global Contiguous Flash Droughts: From an Event-based Spatiotemporal Perspective. Journal of Hydrology, 133934.
46. Li, Wantong, Pacheco-labrador, Javier, Migliavacca, Mirco, Miralles, Diego, Dijke H.V., Anne, Reichstein, Markus, Forkel, Matthias, Zhang, Weijie, Frankenberg, Christian, Panwar, & Annu. (2023). Widespread and Complex Drought Effects on Vegetation Physiology Inferred From Space. Nature Communications, 14(1), 4640.
47. Lundberg, M S., Lee, & Su-in. (2017). A Unified Approach to Interpreting Model Predictions. Advances in Neural Information Processing Systems, 30.
48. Rusjan, Simon, Sapač, Klaudija, Petrič, Metka, Lojen, Sonja, Bezak, & Nejc. (2019). Identifying the Hydrological Behavior of a Complex Karst System Using Stable Isotopes. Journal of Hydrology, 577, 123956. https://www.sciencedirect.com/science/article/pii/S0022169419306766. https://doi.org/10.1016/j.jhydrol.2019.123956.
49. Cui Y., Zhang B., Huang H., Zeng J., Wang X., & Jiao W.. (2021). Spatiotemporal Characteristics of Drought in the North China Plain Over the Past 58 Years. Atmosphere, 12, 844. https://doi.org/10.3390/atmos12070844. 10.3390/atmos12070844.
50. Jiang, Linwei, Gao, Wenhao, Zhu, Kexu, Zheng, Jianqiu, Ren, & Baohua. (2025). Why Did the Extreme Drought in the Yangtze River Basin in 2022 Break the 2019 Record?. Earth and Space Science, 12(3), e2024EA003972.
51. Yuan, Xing, Wang, Yumiao, Ji, Peng, Wu, Peili, Sheffield, Justin, Otkin, & A J.. (2023). A Global Transition to Flash Droughts Under Climate Change. Science, 380(6641), 187-191.
52. Jing Y., Wang S., Chan P.W., & Yang Z.. (2025). Gross Primary Productivity Is More Sensitive to Accelerated Flash Droughts. Communications Earth & Environment, 6. https://doi.org/10.1038/s43247-025-02013-w. 10.1038/s43247-025-02013-w.
53. Jia, Qianlan, Liu, Zhunqiao, Guo, Chenhui, Wang, Yakai, Yang, Jingjing, Yu, Qiang, Wang, Jing, Zheng, Fenli, Lu, & Xiaoliang. (2023). Relationship Between Photosynthetic Co2 Assimilation and Chlorophyll Fluorescence for Winter Wheat Under Water Stress. Plants, 12(19), 3365.
54. Beauclaire, Quentin, Heinesch, Bernard, Longdoz, & Bernard. (2023). Non-stomatal Processes Are Responsible for the Decrease in Gross Primary Production of a Potato Crop During Edaphic Drought. Agricultural and Forest Meteorology, 343, 109782.
55. Mohammadi, Koushan, Jiang, Yelin, Wang, & Guiling. (2022). Flash Drought Early Warning Based on the Trajectory of Solar-induced Chlorophyll Fluorescence. Proceedings of the National Academy of Sciences, 119(32), e2202767119.
56. Hassan, A M., Dahu, Ni, Hongning, Tong, Qian, Zhu, Yueming, Yi, Yiru, Li, Shimei, & Wang. (2023). Drought Stress in Rice: Morpho-physiological and Molecular Responses and Marker-assisted Breeding. Frontiers in Plant Science, 14, 1215371.
57. Adil, Muhammad, Zhang, Shaohong, Wang, Jun, Shah, Noor A., Tanveer, Mohsin, Fiaz, & Sajid. (2022). Effects of Fallow Management Practices on Soil Water, Crop Yield and Water Use Efficiency in Winter Wheat Monoculture System: a Meta-analysis. Frontiers in Plant Science, 13, 825309.
58. Ma, Yingying, Tang, Mingyue, Wang, Mingyang, Yu, Yanchun, Ruan, & Banpu. (2024). Advances in Understanding Drought Stress Responses in Rice: Molecular Mechanisms of Aba Signaling and Breeding Prospects. Genes, 15(12), 1529.

 doi:10.20944/preprints202605.1263.v1

59. Shi, Ruiguang, Liu, Yi, Zhu, Ye, Ren, Liliang, Liu, Yu, Zhang, Xinyu, Zhang, & Linqi. (2025). Impact of Flash Droughts on Global Crop Yields Considering Crop Phenology and Irrigation Conditions. Agricultural and Forest Meteorology, 373, 110763.
60. Zhao Y., Xiong L., Yin J., Zha X., Li W., & Han Y.. (2024). Understanding the Effects of Flash Drought on Vegetation Photosynthesis and Potential Drivers Over China. Science of the Total Environment, 931, 172926. https://www.sciencedirect.com/science/article/pii/S0048969724030730. 10.1016/j.scitotenv.2024.172926.
61. Yuan, Xing, Wang, Yumiao, Zhou, Shiyu, Li, Hua, Li, & Chenyuan. (2024). Multiscale Causes of the 2022 Yangtze Mega-flash Drought Under Climate Change. Science China Earth Sciences, 67(8), 2649-2660. https://doi.org/10.1007/s11430-024-1356-x. 10.1007/s11430-024-1356-x.
62. Gao, Yun, Hu, Tiesong, Wang, Qin, Yuan, Hongwei, Yang, & Jiwei. (2019). Effect of Drought–flood Abrupt Alternation on Rice Yield and Yield Components. Crop Science, 59(1), 280-292.
63. Chen, Jiana, Cao, Fangbo, Yin, Xiaohong, Huang, Min, Zou, & Yingbin. (2019). Yield Performance of Early-season Rice Cultivars Grown in the Late Season of Double-season Crop Production Under Machine-transplanted Conditions. Plos One, 14(3), e0213075.
64. Jiang, Liangliang, Liu, Wenli, Liu, Bing, Yuan, Ye, Bao, & Anming. (2023). Monitoring Vegetation Sensitivity to Drought Events in China. Science of the Total Environment, 893, 164917.